Prabha Materials Science Letters
Vol. 2, No. 1, 1-15, 2023
https://doi.org/10.33889/PMSL.2023.2.1.001

Enhancement in Thermal Properties of Organic Phase Change Material (Paraffin) via TiO_2 Foam Doping

Neetu Bora
Department of Physics,
Govind Ballabh Pant University of Agriculture and Technology,
Pantnagar, 263145, Uttarakhand, India.
Corresponding author: neetubora95@gmail.com

Deepika P. Joshi
Department of Physics,
Govind Ballabh Pant University of Agriculture and Technology,
Pantnagar, 263145, Uttarakhand, India.
E-mail: deepikakandpal@gmail.com

(Received on February 04, 2023; Accepted on February 17, 2023)

Abstract
Phase change materials (PCM) can absorb or release a huge amount of latent heat in accordance with the increase or decrease of the surrounding temperature. Among all the studied PCMs, organic PCM paraffin has been chosen due to the large energy storage capacity for thermal energy storage (TES). The present work introduces a thermally modified phase change material by TiO_2 foam impregnation in paraffin. Three TiO_2/paraffin PCM composites TPCM1, TPCM2, and TPCM3 containing 10 wt.%, 15 wt.%, and 20 wt.% of TiO_2 foam with paraffin have been successfully synthesized for thermal energy storage. The porous TiO_2 foam can provide a high paraffin loading capacity of up to 80 % (TPCM3) due to hollow cavities. TiO_2 foam is uniformly distributed over the inner and outer surface of the paraffin as a nano additive to enhance the thermal conductivity (TC) of the composite PCM. The structural, morphological, and thermal study revealed that doping of the supporting material has potentially modified all the criteria of PCM composite for TES. The highest leakage-proof result was obtained for 20 wt.% of TiO_2 foam impregnated composite (TPCM3) by analysing mass loss across 500 thermal cycles in an oven at 80°C. The thermal reliability of the TPCM3 composite has also been investigated after 500 thermal cycles. The TPCM3 composite maintains its crystalline nature with homogeneous dispersion and thermal stability without affecting the thermal and chemical properties of the PCM. The latent heat of the TPCM3 composite reached 182.87 J/g, and the thermal conductivity has been calculated at 0.71 W/m-K, which is 3.73 times higher than paraffin. The results concluded that synthesized TPCM3 composite could be a potential candidate for TES due to chemical and physical compatibility, easy synthesis process, good thermal and chemical reliability, and acceptable energy storage capacity with enhanced thermal conductivity.

Keywords- Paraffin, TiO_2 foam, Latent heat, Thermal conductivity, Thermal stability.

1. Introduction

The amount of greenhouse gases significantly increased due to the quick usage of fossil fuels. Since 1751, the amount of carbon dioxide emissions has climbed to over 347 billion tonnes (Prabhu and ValanArasu, 2020). Scientists are therefore making enormous efforts to limit the use of fossil fuels, and to produce energy from renewable sources, such as wind, sunshine, geothermal, and hydropower. Given its abundance and accessibility, solar energy is one of the most promising forms of renewable energy (Prabhu and ValanArasu, 2020; Nie et al., 2021). By 2050, according to the International Energy Agency, solar energy will generate 21 % of the global electricity consumption (Su et al., 2018; Parvate et al., 2021). However, there are many issues with the use of solar energy (Mazinani et al., 2017; Deka et al., 2020). Area, time of day, season, and local meteorological conditions all affect how strong the sun's radiation is at any given location (clear and cloudy sky) (Mitran et al., 2021; Wang et al., 2021). However, bridging

the energy supply and demand gap by employing renewable energy (such wind, solar, and hydroelectric energy) may be seen as a driving factor in this process (Yao et al., 2014). The usage of renewable energy is also subject to some restrictions since it is not always and constantly available (Aulakh and Joshi, 2019). As a result, it makes engineering valuable to store solar energy in various ways, such as electrochemical and thermal energy storage systems (TESS) (Antony et al., 2021). Therefore, the creation of such energy-storing materials that can be used later becomes crucial. In this regard, phase change materials (PCM) have drawn the focus of researchers for thermal energy storage (TES).

There are three different kinds of PCM: eutectic, organic, and inorganic (Prasanna and Deshmukh, 2021). The inorganic PCMs are often hydroxides, alloys, and salt hydrates, which have good thermal conductivity, and latent heat storage capacity. However, unpredictable melting behaviour is less trustworthy (Jebaraj and Iniyan, 2006; Mazinani et al., 2017; Prasanna and Deshmukh, 2021). The majority of the organic PCMs are made of fatty acids, and paraffin has been shown potential candidate as a TES material due to its non-toxic and higher latent heat storage (LHS) fusion capability (Deka et al., 2020; Zhang et al., 2020). For TES, organic PCMs (particularly paraffin) have drawn the most attention out of all the identified PCMs since they can absorb or release a significant quantity of latent heat in response to changes in ambient temperature (Son et al., 2013). Therefore, paraffin has a considerable capability for storing energy (Li et al., 2014). However, the thermo-physical characteristics of paraffin (such as shape, structure, thermal conductivity, reliability, thermal deterioration, and thermal performance) have not been able to meet all of the demands of engineers for TES devices (Hou et al., 2011). To improve the understanding of the thermo-physical characteristics of paraffin, many investigations have been carried out. A review of the literature found that dispersing metal, and their oxide nanoparticles (NPs) in paraffin, such as TiO_2, CuO, ZnO, SiO_2, etc., can significantly increase the thermal properties and the thermal conductivity of paraffin (Singh, 2019; Zhou et al., 2020; Wang et al., 2021).

Zhou et al. (2020) reported the synthesis of TiO_2 NPs by a facile gas flame combustion method. It has been found that the synthesized TiO_2 NPs show an anatase phase with a particle size of about 9 nm. Chen et al. (2020) prepared new three-dimensional interconnected hierarchically porous anatase TiO_2 foam with the mesoporous wall structure, via a sol-gel templating method. Zhu et al. (2022) reported the synthesis of TiO_2 NPs by sol-gel method, and found that TiO_2 NPs have excellent chemical and thermal stability, and the band gap and surface area were calculated to be 3.2 eV and 64.041 m^2/g. Nomura et al. (2015) successfully developed the sol-gel synthesis method for TiO_2 nanoparticles. Khannyra et al. (2022) conducted rutin mediated synthesis method for the development of TiO_2 nanoparticles (NPs). XRD showed the amorphous nature of titanium dioxide nanoparticles . Mahdi and Kara (2021) successfully prepared nano-TiO_2 paraffin composite. It was found that on increasing the TiO_2 content, viscosity, density, thermal conductivity increases. However, the composite shows less thermal stability due to the leakage of paraffin from the prepared composite . The dispersion of SiO_2 NPs, TiO_2 NPs, copolymers, ZnO NPs, CuO NPs, and all other NPs in paraffin shows a slightly improvement in thermal conductivity, leakage, and homogeneity, however with a significant decrease in latent heat (Hsu et al.,1993; Small et al., 2005; Wang et al., 2021). To build the optimum material for TES, it is necessary to create shape-stable paraffin composite with high latent heat and high thermal conductivity.

Hence, the present work attempts to develop a novel kind of shape-stable phase change composite material by using TiO_2 foam with paraffin to prevent leakage problems, and enhance the thermal stability, reliability, and conductivity of paraffin. For achieving all these properties, titanium dioxides (TiO_2) foam have been synthesized (Khannyra et al., 2022). Titanium dioxide (TiO_2) semiconductor nanoparticles, a classic inorganic metal oxide material that naturally occurs on the earth and it has a different crystal structure rutile, anatase, and brookite (Hsu et al., 1993; Mahdi and Kara, 2021). Due to their PH

dependence (~1.5), TiO_2 nanoparticles form aggregated cluster-type and tetragonal structures as shown in Figure 1 (Small et al., 2005). Anatase TiO_2 NPs have a relevant band gap of 3.23 eV, while rutile has a band gap of 3.06 eV (Hairom et al., 2021). Metal oxide has been used as a shell matrix due to its thermal conductivity promoter property, porous nature, non-toxic, and relatively cost-effective in comparison to other metals and metal oxides (Kandpal et al., 2007; Sharma et al., 2022). In addition to these, TiO_2 is nonreactive with organic PCM (Sharma et al., 2009; Mugundan et al., 2022; Razak et al., 2022). Synthesized TiO_2 foam has been used for preparing TiO_2/paraffin composites via direct mixing of TiO_2 in paraffin with various wt.% (i.e., 10 %, 15 %, and 20 %). Direct mixing synthesis is a low-cost, facile, and very effective method for preparing paraffin composites. Different techniques have been used to characterize the manufactured TES materials, including the Leakage test, XRD, FESEM, FTIR, DSC, TGA, and LFA.

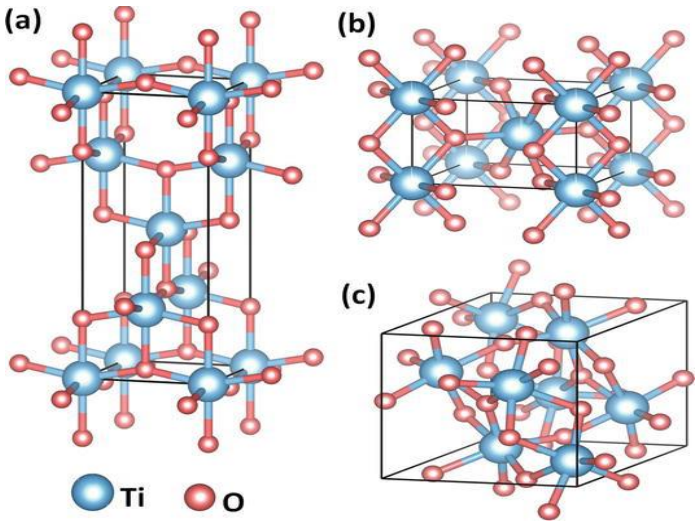

Figure 1. Crystal structure of TiO_2 (a) Anatase (tetragonal) (b) Rutile (tetragonal) (c) Brookite (orthorhombic) micrograph.

2. Materials and Method

2.1 Materials Used

Chemical used in this experiment, are Titanium (IV) iso-propoxide (TTIP, 98+%), purchased from Sigma Aldrich. Acetonitrile (98 %), ammonium hydroxide (29 % in water), absolute ethanol (99.5 %), and paraffin have been received from Hi-media. Distilled water (DI water) used in experiment, collected from laboratory water distiller.

2.2 Synthesis of TiO_2 Foam

TiO_2 foam has been synthesized via the Sol-gel method as shown in Figure 2. First TTIP is added dropwise with ethanol and water with continuous stirring. Using diluted H_2SO_4 to keep the PH at 1.5, 4 moles of water have been added to the solution after 35 minutes, and the mixture then magnetically agitated for 45 minutes at 1200 rpm. A gel-like solution has been obtained after 50 minutes it has been treated at 130°C for one hour. Yellow-coloured particles have been received, and washed with DI water. Further, the washed particles have been centrifuged at 10,000 rpm, and the obtained light yellow-coloured foamy particles have been dried at 60°C in hot air oven (Su et al., 2018; Mazinani et al., 2017; Deka et al., 2020). The final TiO_2 foam has been obtained after being calcinated at 450°C for 2:30 hours.

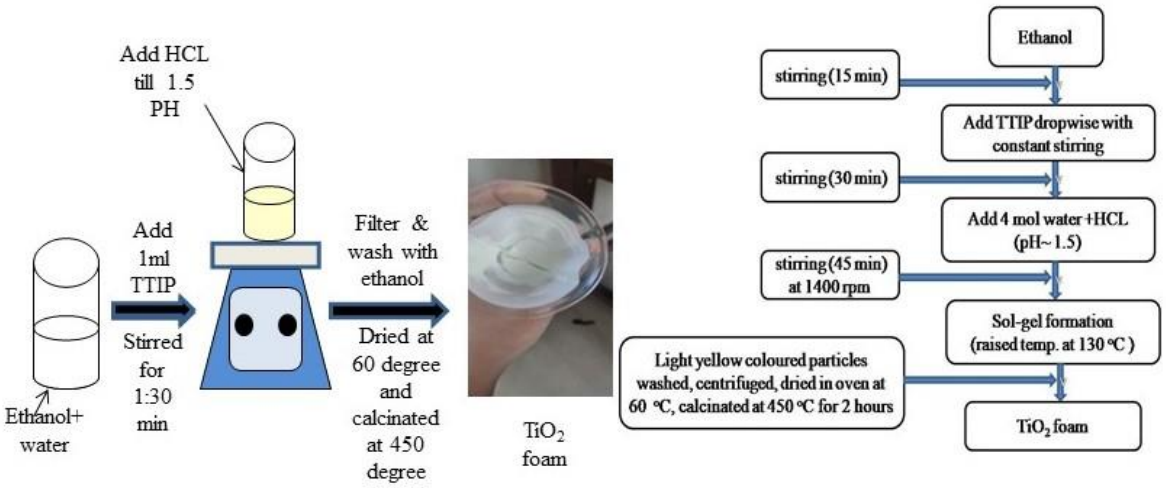

Figure 2. Schematic block diagram of the synthesis of TiO_2 foam.

2.3 Synthesis of TiO_2/Paraffin Composite

Paraffin wax has been melted at 65°C in a water bath. An analytical microbalance has been used to measure the wt.% of the synthesised TiO_2 foam (10 %, 15 %, 20 %). After adding TiO_2 foam to the heated paraffin wax stirred for 1 hour, after stirring the probe sonication has been performed for 30 minutes. After sonication, the TiO_2/paraffin composite has been allowed to cool at ambient temperature (Hairom et al., 2021). Finally, samples have been moulded in a hydraulic press with a diameter of 10.2 mm and a thickness of 3 mm. In this way, a series of composite PCMs have been prepared, which contain 10 wt.%, 15 wt.%, and 20 wt.% of TiO_2 foam in paraffin viz. TPCM1, TPCM2, and TPCM3, respectively. Schematic block diagram of the synthesis of TiO_2/paraffin composite has been summarized in Figure 3.

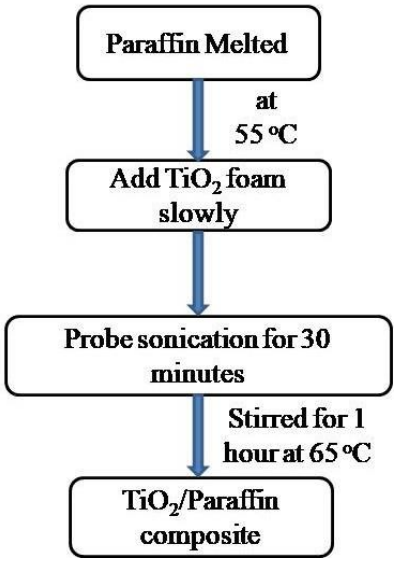

Figure 3. Schematic block diagram of the synthesis of TiO_2/paraffin composites.

Using X-ray light at the 2θ range from an XRD (X-ray diffractometer), the crystal structure of TiO_2 foam has been studied at 10^o to 80^o. Fourier transformation infrared spectroscopy (FTIR) has been used to analyze the chemical composition of TiO_2 foam (FTIR, Bruker, 600-4000 cm^{-1}). Field emission scanning microscope (FESEM) is used to conduct the morphological assessment. The seepage test has been conducted to determine the TPCM3 composite's trustworthiness and reusability.

3. Result and Discussion

3.1 Leakage Test

The current work is an attempt to investigate the leakage-bearing property of various synthesized PCM composites. To achieve minimal paraffin leakage for many TES applications, the ratio of impregnation of prepared TiO_2 foam in paraffin has been optimized through the leakage test. That modifies the leakage property of paraffin and convert it into a shape stable PCM for TES applications.

The leakage performance and shape stability of produced composite samples have been assessed by placing the TPCM1, TPCM2, and TPCM3 samples in a hot air oven set at 80^oC. The samples are thermally treated for 500 thermal cycles while being wrapped in filter paper.

3.1.1 Seepage Analysis

The formula used to determine the paraffin leakage rate, is denoted by Equation 1 (Aulakh and Joshi, 2019).

$$L = \frac{W_o - W_n}{W_o} \times 100\% \quad (1)$$

where, W_o and W_n are the weight of the sample before and after thermal treatment.

Figure 4 displays the weight loss curves for the sample TPCM1, TPCM2, and TPCM3, which shows the leakage rate, is 0.77 %, 0.40 %, and 0.08 %, respectively. The TPCM3 sample shows negligible leakage of 0.08 % of paraffin due to the porous nature of TiO_2 Foam. Paraffin is absorbed into the porous structure of TiO_2, and so this cross-linked network-like shape limits paraffin's momentum within the matrix. Therefore, a certain rigidity caused by TiO_2 foam has effectively stopped the smooth running of paraffin when the temperature is increased over the melting point of paraffin (Khannyra et al., 2022). Additionally, the inclusion of TiO_2 foam shows a favourable impact on the paraffin composite's leakage tendency (Hairom et al., 2021). It can help to improve the leakage problem during the phase change process and stabilize the PCM due to the surface tension, capillary force, and other interactions between the porous network of TiO_2 foam and PCM (Yao et al., 2014). Figure 4 makes it abundantly evident that there is no sign of leakage in the filter paper surrounding the composites after numerous heat treatment cycles, which is a positive finding for establishing the leakage-proof PCM successfully.

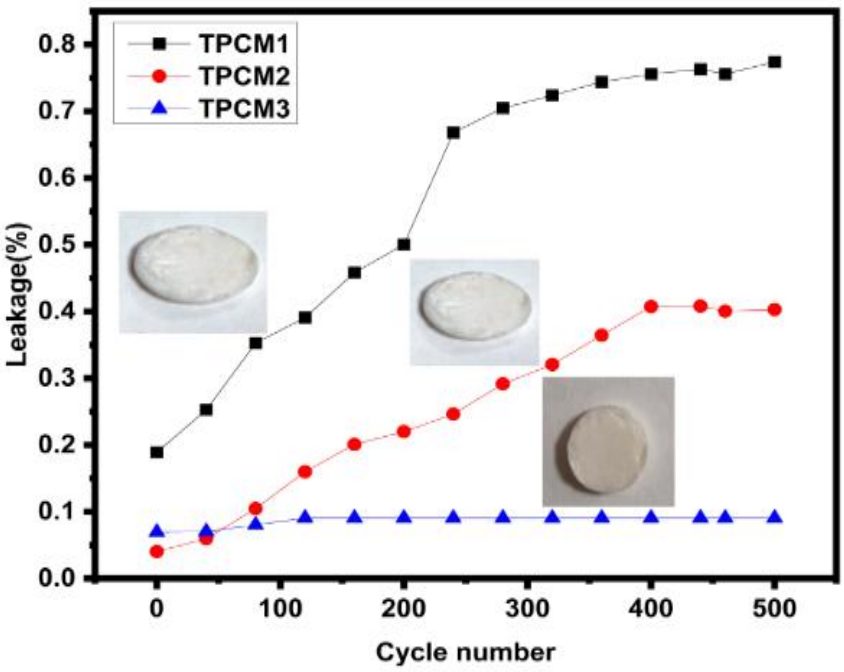

Figure 4. Leakage test analysis of TPCM1, TPCM2 and TPCM3 composites.

3.2 XRD Analysis

To investigate the crystalline property of the TiO_2 foam, paraffin and TiO_2/paraffin composite (TPCM3), XRD has been performed. The results are presented in Figure 5 (a), (b) & (c) respectively). The diffractogram for TiO_2 foam shows sharp peaks at (110), (101), (200), (111), (210), (211), (220), (002), (310), (301), (112). This confirms the anatase phase and rutile phase of TiO_2 foam at 450°C temperature which are in good agreement with the literature (Zhou et al., 2020). Paraffin shows two sharp and intense diffraction peaks at miller indices (110) and (200), respectively and some other small peaks which show the crystalline nature of pure paraffin wax. According to the XRD data of TiO_2/paraffin (TPCM3) composite materials, all of the miller indices (110, 110), (101), (200), (111), (210), (211), (220), (002), (310), (301), and (112) diffraction peaks of TiO_2 foam and paraffin are present in the TPCM3 composites, and no additional new peaks are found (Mahdi and Kara, 2021). It suggests that there is not any chemical interaction between paraffin and TiO_2 foam.

Utilizing the following formulas, the average crystallite size, strain, and dislocation density of the samples have been determined (Antony et al., 2021).

$$D = \frac{k\lambda}{\beta cos\theta} \quad (2)$$

$$\varepsilon = \frac{\beta}{4\, tan\theta} \quad (3)$$

$$\delta = \frac{1}{D^2} \quad (4)$$

where, β, D, ε, δ, θ, k, and λ are the full width at half maximum (FWHM) of the peaks, average crystallite size, strain due to distortions, contents of dislocations, Bragg's angle, shape function (0.98) and X-ray wavelength (1.541Å), respectively.

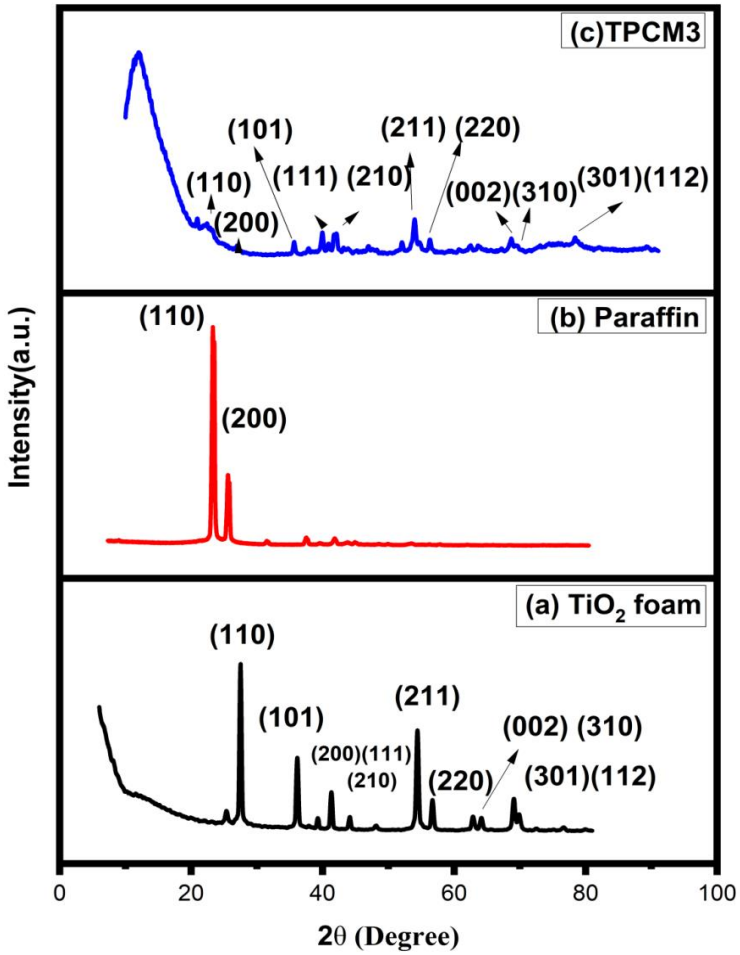

Figure 5. XRD patterns of (a) TiO_2 foam, (b) paraffin and (c) TPCM3 composite.

For TiO_2 foam, average crystallite size has been estimated at approximately 17.07 nm. This shows that TiO_2 foam has a finer structure. In addition, it is also observed that as the particle size decreases, the micro-strain increases. The strain, crystallite size, and micro-strain of synthesized samples are tabulated in Table1. The results of XRD initially proved the successful synthesis of the TiO_2 foam.

Table 1. XRD data of TiO_2 foam.

Compound	Crystalline size (nm)	Micro-strain (10^{-3})	Dislocation density ($\delta \times 10^{-3}$)
TiO_2 foam	17.07	1.61	0.343
Paraffin	16.5	0.859	0.367
TPCM3	17.2	0.99	0.338

3.3 FTIR Analysis

Figure 6 (a), (b), & (c) respectively) shows the infrared (IR) spectra of TiO_2 foam, paraffin, and TPCM3 composite, respectively. The spectrum of the TiO_2 foam, as shown in Figure 6(a), represents the stretching spectra of Ti-O and Ti-O-Ti with a distinctive wide band at 500-700 cm^{-1}. The stretching vibrations of -

CH_2 and -CH_3 could be attributed to the absorption peaks in the paraffin FTIR spectrum at 2917.95 cm^{-1} and 2852.64 cm^{-1}, while the stretching vibration of C=O could be attributed to the absorption peak at 1681.39 cm^{-1} (Li et al., 2014). The absorption peaks at 1536.51 cm^{-1} and 714 cm^{-1} might be attributed to -CH3 in-plane bending and swing vibrations, respectively. The IR spectra of the TPCM3 composite may be seen to contain the entire features of TiO_2 foam and paraffin. However, the TPCM3 composite shows no new distinctive absorption bands, indicating that the absorption of paraffin into the porous TiO_2 foam network is just a physical contact and not a chemical reaction. This conclusion is further corroborated by the XRD results.

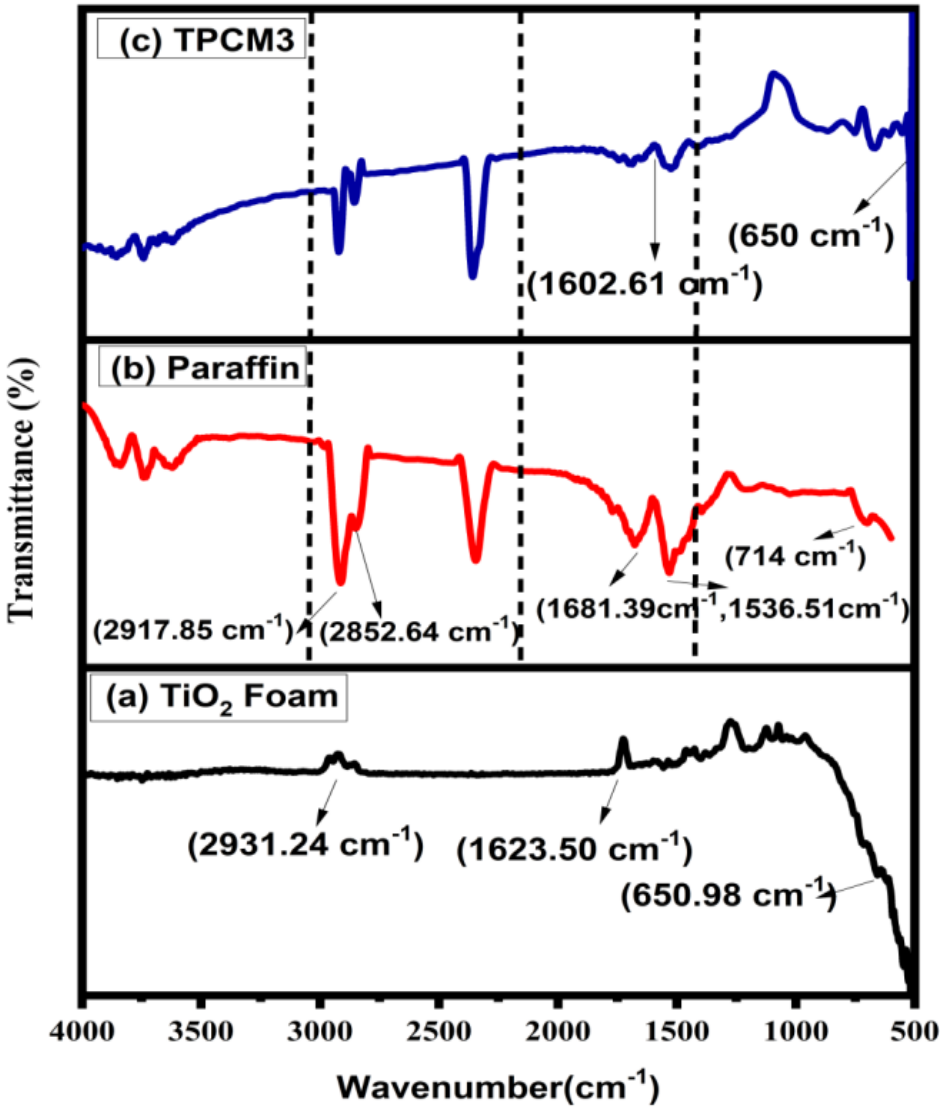

Figure 6. FTIR analysis of the samples (a) TiO_2 foam (b) paraffin and (c) TPCM3 composite.

3.4 FESEM Analysis

The surface morphologies of the TiO_2 foam and TPCM3 composite are shown in Figure 7 (a) & (b). TiO_2 foam has a typically porous foam/cluster like structure as shown in Figure 7 (a). It contains several regular tetragonal networks (Figure 1) and reticulates pores on the surface, which shows consistency with the existing literature of TiO_2 foam (Chen et al., 2020; Zhou et al., 2020). The rich micro pore structure of the TiO_2 foam has relatively high thermal conductivity, excellent chemical stability, and the robust mechanical properties make it a better candidate material for thermal energy storage (Zhang et al., 2020). Figure 7 (b) depicts the surface morphology of the TPCM3 composite; it is evident that after adding paraffin into TiO_2 foam, the surface structure of TiO_2/paraffin composite has become regular. A similar-phenomenon is observed by other researchers (Hairom et al., 2021). As a result, there is no sign of immiscibility between TiO_2 foam and paraffin in the FESEM pictures, indicating that the uniform paraffin dispersion into the TiO_2 network is required for creating leakage-proof PCM.

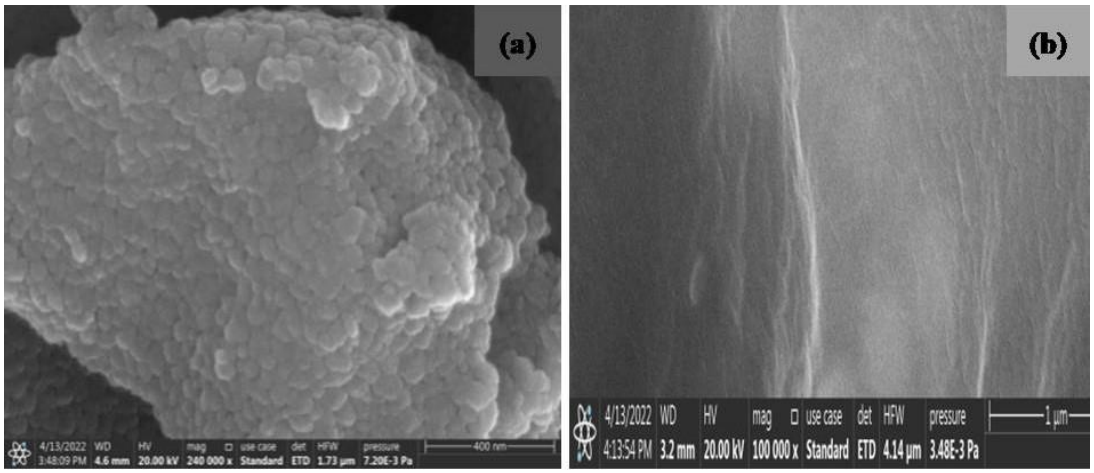

Figure 7. FESEM images (a) TiO_2 foam (b) TPCM3 composite.

3.5 Thermal Stability

The thermal stability of composite PCMs has been analysed using thermogravimetry (TGA). Figures 8(a) and 8(b) show the TGA and DTG (Derivative thermogravimetry analysis) curves of paraffin and TPCM3 composites, respectively. The weight loss curve of paraffin and TPCM3 composites exhibits one-step heat degradation, as can be shown in Figure 8 (a). Paraffin began to degrade thermally at about 220°C and is fully destroyed at 350°C. The DTG curve is depicted in Figure 8 (b), and at 345°C, the highest degradation rate has been noted (Hairom et al., 2021). The TGA profile of the TPCM3 sample shows one-step degradation up to 600ºC, which is typical for immiscible mixes with various degradation temperatures. The first step, corresponding to paraffin degradation, starts at roughly 150°C and ends at roughly 380°C. The amount incorporated in the composites, is proportional to the rate of weight reduction throughout this phase. The TGA in this study has been conducted between 27 and 600 degrees Celsius, and as indicated in Figure 8 (a), the residue in the TPCM3 composite can be recognised as TiO_2 foam. The residue amount and the wt.%. of TiO_2 foam in the TiO_2/paraffin (TPCM3) composite are comparable. In light of these findings, it can be concluded that PCM is effectively synthesised and has great thermal stability up to 80ºC.

Additionally, the maximal breakdown (DTG) rate for paraffin and TPCM3 is revealed by the DTG curve of composite around 1.76 mg/min, and 1.35 mg/min at temperatures 345ºC and 330ºC, respectively. It has been observed that TiO_2 foam has a positive effect on the degradation of composite resulting in a substantial rise in the degradation temperature. This might be because the porous TiO_2foam network slows down the process of deterioration, and increases the thermal stability of composites by hindering the release of volatile paraffin (Hairom et al., 2021). Table 2 contains the DTG overview of PCM blends.

Table 2. Specific data of TGA/DTG curve.

Sample	T_{onset} (ºC)	T_{offset}(ºC)	Δw(%)	DTG(mg/min)	Residue (%) (600°C)
Paraffin PCM	200 ± 0.20	350 ± 0.20	100	1.76	0
TPCM3	240 ± 0.20	380 ± 0.20	80	1.35	20

where, T_{onset}, T_{offset}, and Δw (%) denotes onset degradation temperature, offset degradation temperature, and paraffin wt.% in the sample.

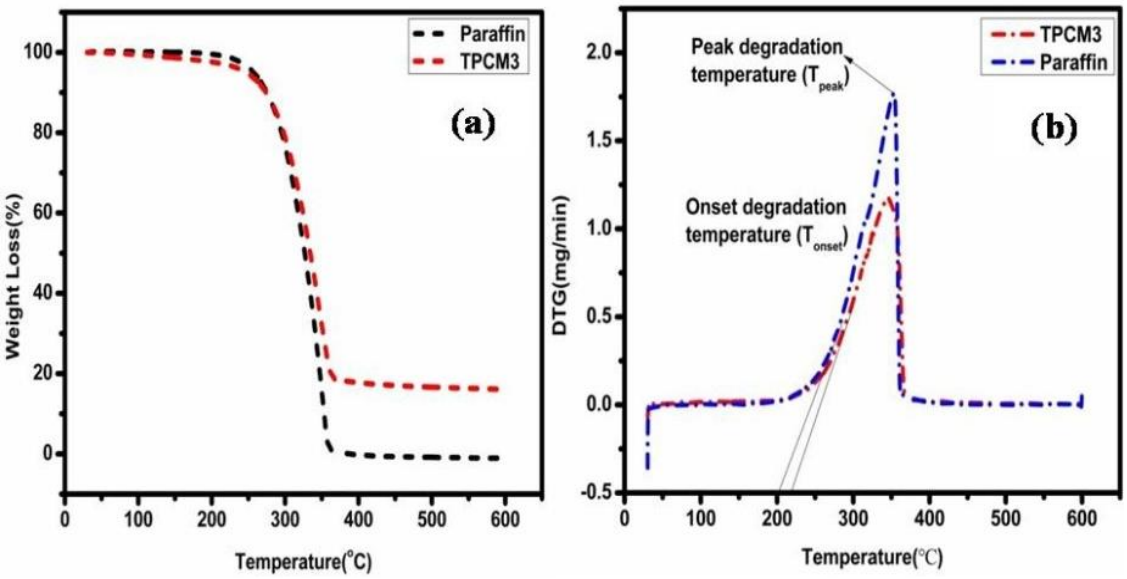

Figure 8. (a) TGA and (b) DTG curves for paraffin and TPCM3 composite.

3.6 DSC Results

Through DSC analysis, the phase - transition properties of paraffin and the compositions made from TiO_2 foam have been investigated. Figure 9 (a) & (b) depict the findings of the heating and cooling images obtained, and Table 3 summarises the relevant parameters obtained from DSC measurements. As seen in the picture, paraffin has two transition region peaks: the first at around 36.90-50.20ºC for solid-solid phase transition and the second at around 52.23-69.77ºCfor liquid phase change process. During phase transition process, the main peak around 62.77ºC may be traced to the heterogeneously nucleated rotator liquid. It indicates the paraffin's strong solid-liquid phase transformation. The peak to the left of the primary peak results from a change in the homogeneously nucleated crystal rotator, which shows that paraffin's solid-solid phase, has been adjusted (Chen et al., 2020; Zhu et al., 2022). Most likely, this peak is associated with the rebuilding of the orthorhombic to the hexagonal crystal structure, which often occurs in various paraffin waxes.

The TPCM3 composite has been heated during the DSC test from ambient temperature to 600°C. For the composite comprising 20 wt.% of TiO_2 foam, the exothermic process has been seen. The melting/freezing peak temperatures of paraffin andTPCM3 composite have been observed around 62.77°C/ 52.52°C, and 63.3°C /55.96°C, respectively. TPCM3 composites peak temperatures differ slightly from those of pure paraffin. This variation is caused by the entrapment of the liquid paraffin into the porous network of TiO_2foam. The Gibbs-Thomson equation, which describes the pore size of a porous material, significantly impacts on the phase change temperature of PCM (Sharma et al., 2022).

$$\Delta T \propto \frac{1}{r-t} \tag{5}$$

where, ΔT is the difference in melting temperature (due to shifting), t is the PCM thickness in pores, and r is pores radius. ΔT has an inverse relationship with r, therefore, melting temperature is depressed with increasing pore size (Jebaraj and Iniyan, 2006; Prabhu and ValanArasu, 2020).

Additionally, the latent heat storage capacities of pure paraffin, and TPCM3 composite during the melting/freezing processes have been found 224/195.5 J/g, and 182.87/113.62 J/g, respectively.

The incorporation rate (%) of paraffin in TPCM3 has been calculated by using the relation (Prabhu and ValanArasu, 2020).

$$\eta(\%) = \frac{\Delta L_{com}}{\Delta L_{para}} \times 100\% \tag{6}$$

where,
η -Incorporation rate (wt.%),
ΔL_{com}- Latent heat of composite,
ΔL_{para}- Latent heat of pure paraffin.

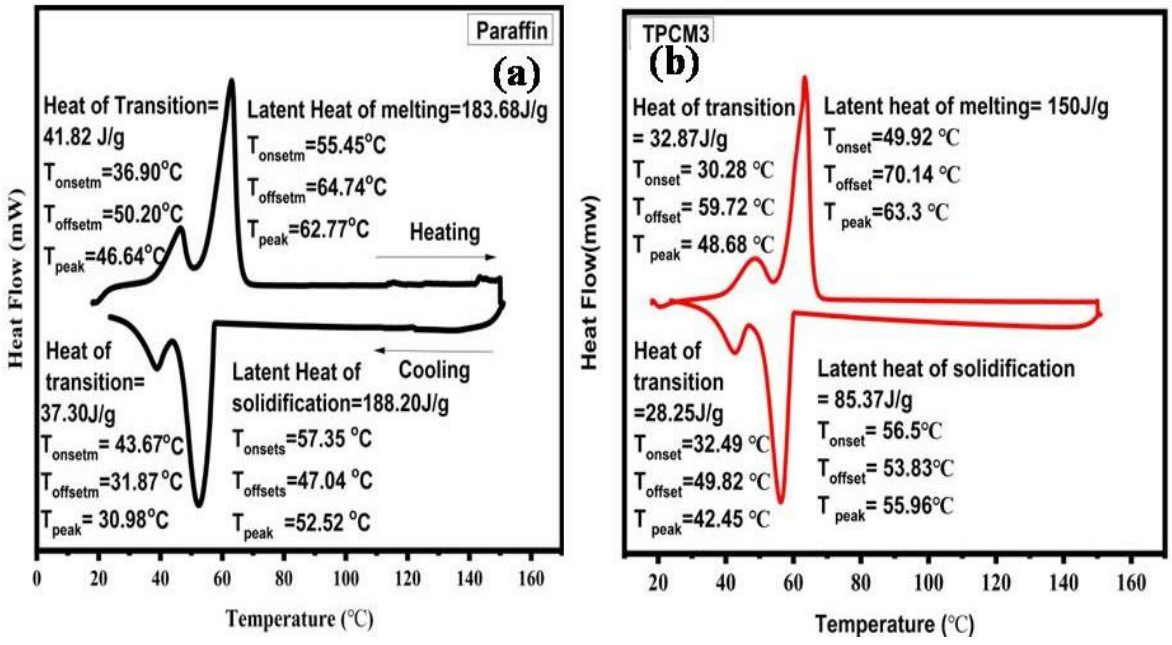

Figure 9. DSC profiles of melting and solidification curve (a)Paraffin (b) TPCM3 composite.

The impregnation of TiO_2 foam into paraffin has not shown any positive effect on latent heat. However, there is a small decrement in latent heat. That is admissible in comparison to thermal property enhancement. In the Table 3 and Table 4, some thermal properties, such as the peak temperature and latent heat of pure paraffin and TPCM3composite for melting and solidification process have been reported and compared.

Table 3. DSC results of heating of Paraffin, TPCM3 composite.

Sample	T_{peak}(°C)	T_m (°C)		$\Delta H_{p.Expm}$ J/g	$\Delta H_{p.theoritical}$ J/g	Encapsulation Ratio (%)	Encapsulation Efficiency (%)
		T_{onsetm}	$T_{offsetm}$				
Paraffin	62.77	36.90	64.74	224	225	-	-
TPCM3	63.3	30.28	70.14	182.87	-	81.61	.76

Here, T_{peak} is melting peak temperature, T_m melting temperature, T_{onsetm} and $T_{offsetm}$ are melting onset and offset temperature during solidification process. $\Delta H_{p,exps,}$ and $\Delta H_{p.theoriticals}$ are latent heat; Exp- Experimental; Theoretical during solidification process.

Table 4. DSC results of cooling of paraffin, TPCM3 composite.

Sample	T_{peak}(°C)	T_s(°C)		$\Delta H_{p.Exps}$ J/g	$\Delta H_{p.theoritical}$ J/g
		T_{onsets}	$T_{offsets}$		
Paraffin	52.52	43.67	47.04	195.5	225
TPCM3	55.96	56.5	49.82	113.78	-

where, T_{peak} is melting peak temperature, T_m is melting temperature, T_{onsets} is melting onset temperature, and $T_{offsets}$ is melting offset temperature during solidification process. $\Delta H_{p,exps}$ and $\Delta H_{p.theoriticals}$ are latent heat; Exp- Experimental; Theoretical during solidification process.

3.7 Thermal Conductivity

Thermal conductivity of the pure paraffin PCM and TPCM3 composite have been investigated through the LFA method. The calculated value of the thermal conductivity for TPCM3 composite is found to be increased from 0.19 W/m°C to 0.71 W/m°C in comparison to pure paraffin . The thermal conductivity is calculated by equation 7.

$$K = \alpha \rho C_p \quad (7)$$

where, α= Thermal diffusivity, ρ=Density, C_p= Specific heat, K=Thermal conductivity

Table5. Thermal diffusivity, density, specific heat has been obtained from LFA.

Sample	Diffusivity (mm^2/sec)	Specific heat (J/g/K)	Density(g/cm^2)	Thermal Conductivity (W/m°C)
Paraffin	0.171±0.003	2.1	0.54	0.19
TPCM3	0.181±0.002	0.99	3.96	0.71

4. Conclusions

In present work, the TPCM3 composite has been synthesised via a direct adsorption approach using three different wt.% of TiO_2 foam with paraffin as samples TPCM1 (10 %), TPCM2 (15 %), and TPCM3 (20 %). The leakage performance of sample TPCM3 (20 %) has been found the best compared to all three samples.

From the seepage test 0.08 % leakage of paraffin has been found. Therefore, this sample has been studied for its structural, morphological, and thermal properties. FESEM images confirm the cluster/foam formationTiO_2. The DSC measurement shows that for TPCM3 composite, the change in melting and solidification temperature are 62.77/64.44ºC and 52.52/51.58ºC, respectively, however it shows slight reduction in latent heat as compared to pure paraffin. The presence of TiO_2 foam in paraffin leads to an increase in the conductivity from 0.19 W/mºC to 0.71 W/mºC. The integration of TiO_2 foam increases the thermal stability of PCM due to its porous structure.

Finally, it can be concluded that the proposed material TPCM3 has the great potential to be a better material for storing thermal energy in solar air/water heating systems, building comforts applications.

Conflict of Interest
No potential conflict of interest was reported by the author(s).

Acknowledgements
The authors would like to thank the DES (Director of Experiment Station) G. B. Pant University of Agriculture and Technology, Pantnagar, India for providing financial support for conducting the research work.

References

Antony, A.J., Kala, S.M.J., Joel, C., Bennie, R.B., & Praveendaniel, S. (2021). Enhancing the visible light induced photocatalytic properties of WO3 nanoparticles by doping with vanadium. *Journal of Physics and Chemistry of Solids*, *157*, 110169.

Aulakh, J.S., & Joshi, D.P. (2019). Thermal and heat transfer performance of leakage-proof phase change material. *Journal of Emerging Technologies and Innovative Research*,*6*(2),176-179.

Chen, X., Tang, Z., Liu, P., Gao, H., Chang, Y., & Wang, G. (2020). Smart utilization of multifunctional metal oxides in phase change materials. *Matter*, *3*(3), 708-741.

Deka, P.P., Ansu, A.K., Sharma, R.K., Tyagi, V.V., & Sarı, A. (2020). Development and characterization of form-stable porous TiO2/tetradecanoic acid based composite PCM with long-term stability as solar thermal energy storage material. *International Journal of Energy Research*, *44*(13), 10044-10057.

Hairom, N.H.H., Soon, C.F., Mohamed, R.M.S.R., Morsin, M., Zainal, N., Nayan, N., Zulkifli, C.Z., & Harun, N. H. (2021). A review of nanotechnological applications to detect and control surface water pollution. *Environmental Technology & Innovation*, *24*, 102032.

Hou, Y., Vidu, R., & Stroeve, P. (2011). Solar energy storage methods. *Industrial & Engineering Chemistry Research*, *50*(15), 8954-8964.

Hsu, W.P., Yu, R., & Matijević, E. (1993). Paper whiteners: I. Titania coated silica. *Journal of Colloid and Interface Science*, *156*(1), 56-65.

Jebaraj, S., & Iniyan, S. (2006). A review of energy models. *Renewable and Sustainable Energy Reviews*, *10*(4), 281-311.

Kandpal, D., Kalele, S., & Kulkarni, S.K. (2007). Synthesis and characterization of silica-gold core-shell (SiO_2@Au) nanoparticles. *Pramana - Journal of Physics*, *69*, 277-283.

Khannyra, S., Luna, M., Gil, M.A., Addou, M., & Mosquera, M. J. (2022). Self-cleaning durability assessment of TiO2/SiO2 photocatalysts coated concrete: Effect of indoor and outdoor conditions on the photocatalytic activity. *Building and Environment*, *211*, 108743.

Li, H., Chen, H., Li, X., & Sanjayan, J.G. (2014). Development of thermal energy storage composites and prevention of PCM leakage. *Applied Energy*, *135*, 225-233.

Mahdi, M.T., & Kara, I.H. (2021). Thermophysical characteristic of nano –TiO_2 paraffin wax composite material. *Journal of Mechanical Engineering Research and Development, 44*(6), 48-58.

Mazinani, B., Beitollahi, A., Masrom, A.K., Samiee, L., & Ahmadi, Z. (2017). Synthesis and photocatalytic performance of hollow sphere particles of SiO2-TiO2 composite of mesocellular foam walls. *Ceramics International*, *43*(15), 11786-11791.

Mitran, R.A., Ioniţă, S., Lincu, D., Berger, D., & Matei, C. (2021). A review of composite phase change materials based on porous silica nanomaterials for latent heat storage applications. *Molecules*, *26*(1), 241.

Mugundan, S., Praveen, P., Sridhar, S., Prabu, S., Mary, K.L., Ubaidullah, M., Shaikh, S.F., & Kanagesan, S. (2022). Sol-gel synthesized barium doped TiO2 nanoparticles for solar photocatalytic application. *Inorganic Chemistry Communications*, *139*, 109340. https://doi.org/10.1016/j.inoche.2022.109340.

Nie, C., Liu, J., & Deng, S. (2021). Effect of geometry modification on the thermal response of composite metal foam/phase change material for thermal energy storage. *International Journal of Heat and Mass Transfer*, *165*, 120652.

Nomura, T., Zhu, C., Sheng, N., Tabuchi, K., Sagara, A., & Akiyama, T. (2015). Shape-stabilized phase change composite by impregnation of octadecane into mesoporous SiO2. *Solar Energy Materials and Solar Cells*, *143*, 424-429.

Parvate, S., Singh, J., Dixit, P., Vennapusa, J.R., Maiti, T.K., & Chattopadhyay, S. (2021). Titanium dioxide nanoparticle-decorated polymer microcapsules enclosing phase change material for thermal energy storage and photocatalysis. *ACS Applied Polymer Materials*, *3*(4), 1866-1879.

Prabhu, B., & ValanArasu, A. (2020). Stability analysis of TiO2-Ag nanocomposite particles dispersed paraffin wax as energy storage material for solar thermal systems. *Renewable Energy*, *152*, 358-367.

Prasanna, Y.S., & Deshmukh, S.S. (2021). Significance of Nanomaterials in solar energy storage applications. *Materials Today: Proceedings*, *38*, 2633-2638.

Razak, K.A., Halin, D.C., Abdullah, M.M.A., Salleh, M.M., Mahmed, N., Azani, A., & Chobpattana, V. (2022). Factors of controlling the formation of titanium dioxide (TiO2) synthesized using sol-gel method–a short review. In *Journal of Physics: Conference Series* (Vol. 2169, No. 1, p. 012018). IOP Publishing. Malaysia.

Sharma, A., Tyagi, V.V., Chen, C.R., & Buddhi, D. (2009). Review on thermal energy storage with phase change materials and applications. *Renewable and Sustainable Energy Reviews*, *13*(2), 318-345.

Sharma, R., Kumar, R., Sharma, D.K., Sarkar, M., Mishra, B.K., Puri, V., Priyadarshini, I., Thong, P.H., Ngo, P.T.T., & Nhu, V.H. (2022). Water pollution examination through quality analysis of different rivers: a case study in India. *Environment, Development and Sustainability*, *24*, 7471-7492.

Singh, R.P. (2019). Nanocomposites: Recent trends, developments and applications. In: Singh, R.P. (ed) *Advances in Nanostructured Composites* (pp. 16-47). Boca Raton.

Small, A., Hong, S., & Pine, D. (2005). Scattering properties of core–shell particles in plastic matrices. *Journal of Polymer Science Part B: Polymer Physics*, *43*(24), 3534-3548.

Son, S., Hwang, S.H., Kim, C., Yun, J.Y., & Jang, J. (2013). Designed synthesis of SiO2/TiO2 core/shell structure as light scattering material for highly efficient dye-sensitized solar cells. *ACS Applied Materials & Interfaces*, *5*(11), 4815-4820.

Su, X., Jia, S., Lv, G., & Yu, D. (2018). A unique strategy for polyethylene glycol/hybrid carbon foam phase change materials: morphologies, thermal properties, and energy storage behavior. *Materials*, *11*(10), 2011.

Wang, T., Liu, Y., Meng, R., & Zhang, M. (2021). Thermal performance of galactitol/mannitol eutectic mixture/expanded graphite composite as phase change material for thermal energy harvesting. *Journal of Energy Storage*, *34*, 101997.

Yao, Q., Lu, Z.H., Zhang, Z., Chen, X., & Lan, Y. (2014). One-pot synthesis of core-shell Cu@ SiO2 nanospheres and their catalysis for hydrolytic dehydrogenation of ammonia borane and hydrazine borane. *Scientific Reports*, *4*, 7597. https://doi.org/10.1038/srep07597.

Zhang, W., Tian, Y., He, H., Xu, L., Li, W., & Zhao, D. (2020). Recent advances in the synthesis of hierarchically mesoporous TiO2 materials for energy and environmental applications. *National Science Review*, *7*(11), 1702-1725.

Zhou, J., Zhao, J., Cui, Y., & Cheng, W. (2020). Synthesis of bifunctional nanoencapsulated phase change materials with nano-TiO2 modified polyacrylate shell for thermal energy storage and ultraviolet absorption. *Polymer International*, *69*(2), 140-148.

Zhu, L., Opulencia, M.J.C., Bokov, D.O., Krasnyuk, I.I., Su, C.H., Nguyen, H.C., Mohamed, A., Zare, M.H., Zwawi, M., & Algarni, M. (2022). Synthesis of Ag-coated on a wrinkled SiO2@ TiO2 architectural photocatalyst: New method of wrinkled shell for use of semiconductors in the visible light range and penicillin antibiotic degradation. *Alexandria Engineering Journal*, *61*(12), 9315-9334.